Available online at www.sciencedirect.com

ScienceDirect

IFAC PapersOnLine 56-2 (2023) 2096–2101

Patient Spontaneous Effort Estimation in Digital Twin Model with B-spline Function

Qianhui Sun*, J. Geoffrey Chase*, Cong Zhou*, Merryn H. Tawhai, Jennifer L. Knopp*, Knut Möller***, Thomas Hu*, Geoffrey M. Shaw*****

* *Department of Mechanical Engineering; Dept of Mechanical Eng, Centre for Bio-Engineering, University of Canterbury, Christchurch, New Zealand (e-mail: qianhui.sun@pg.canterbury.ac.nz; geoff.chase@canterbury.ac.nz; cong.zhou@canterbury.ac.nz; jennifer.knopp@canterbury.ac.nz; thu66@uclive.ac.nz)*

** *Auckland Bioengineering Institute, The University of Auckland, Auckland, New Zealand (e-mail: m.tawhai@auckland.ac.nz)*

*** *Institute for Technical Medicine, Furtwangen University, Villingen-Schwenningen, Germany (e-mail: Knut.Moeller@hs-furtwangen.de)*

**** *Department of Intensive Care, Christchurch Hospital, Christchurch, New Zealand (e-mail: geoff.shaw@cdhb.health.nz)*

Abstract: Patient work of breathing is of significant clinical interest for several decades. It is particularly relevant when gauging patient-ventilator interaction, patient-specific level of mechanical ventilation (MV) support, and weaning from full support to spontaneous breathing MV modes or off of MV entirely. Current monitoring approaches require additional equipment (usually expensive), well-trained clinicians (to collect and interpret these signals), or/and extra clinical interventions (increases difficulty and cost). This study extends a digital twin model to estimate patient spontaneous breathing effort ($\hat{P}_p$ curve) with a previously proposed model-based estimation method using b-spline functions. Data from 22 patients for two assisted MV modes, NAVA (neurally adjusted ventilatory assist) and PSV (pressure support ventilation), are employed. Estimation results are compared to breathing effort reflected by electrical activity of the diaphragm (EAdi) signals. Physiologically-relevant correlations in identified $\hat{P}_p$ curve area (negative and positive) and EAdi signal can be found in both NAVA and PSV data analysis. While $\hat{P}_p$ curves yield more negative area (larger PRCTneg), the corresponding breaths tend to have lower peak EAdi values and area under curve of EAdi signal (AUC[EAdi]) during inspiration. R^2 values for NAVA data yield an interquartile range (IQR) from 0.31 to 0.68 for peak EAdi versus PRCTneg and 0.40 to 0.61 for AUC[EAdi] versus PRCTneg, respectively. Results differ between NAVA and PSV modes based on poorer patient-ventilator interaction observed in PSV, while the same level of expected physiological relevance is still observed. Overall, the extended digital twin model with b-spline functions to quantify patient-specific inspiratory effort shows promising application in helping guide weaning or changes in MV settings at bedside for assisted breathing modes of MV. In future, the identified $\hat{P}_p$ curves could also potentially be used to replace the need for costly measurement of EAdi signals.

Keywords: Digital Twin; Mechanical ventilation; Neurally adjusted ventilatory assist; Pressure support ventilation; Spontaneous breathing.

1. INTRODUCTION

EAdi (electrical activity of the diaphragm) is one extensively used method to monitor and study respiratory muscles activities with multiple electrodes and a nasogastric tube (Doorduin, J., et al., 2013, Jonkman, A.H., et al., 2020). While effective and reliable, proper positioning and regularly adjustment are necessary to ensure correct recordings (Vargas, M., et al., 2022), requiring more clinician-involved work and training. Other clinically adopt signals, such as esophageal pressure (P_{es}) (Akoumianaki, E., et al., 2014, Telias, I., et al., 2019), have similar technical concerns (Akoumianaki, E., et al., 2014, Jansen, D., et al., 2018). Moreover, most signal monitoring methods requires intubation or additional devices and thus less comfort and convenience for clinical use.

Several researches (physiologically relevant models and derived variables) and clinical tools (invasive and non-invasive measurements) are designed to monitor respiratory drive and respiratory muscle unloading (Albani, F., et al., 2021, Doorduin, J., et al., 2013, Jansen, D., et al., 2018, Knopp, J.L., et al., 2021, Telias, I., et al., 2020), aiming for a better understanding and novel insight for patient lung mechanics interaction with ventilator support. However, they often need additional equipment, well-trained clinicians (to collect and interpret these signals), or extra clinical treatment applications, increasing the difficulty and cost in routinely use.

Non-invasive, derived variables from ventilators are

10.1016/j.ifacol.2023.10.1111

meanwhile studied to offer better or equally effective respiratory muscle activities while minimising cost and inconvenience (Jansen, D., et al., 2018, Telias, I., et al., 2020, Telias, I., et al., 2019). WOB (work of breathing) and PTP (pressure-time product) are mostly considered to be capable to assess respiratory effort (Akoumianaki, E., et al., 2014). However, most of them, including WOB and PTP, are recommended to calculate with Pes or Pdi (transdiaphragmatic pressure) instead of airway pressure (Akoumianaki, E., et al., 2014), which thus still need invasive procedure.

In this study, a digital twin model is extended with b-splines function (Knopp, J.L., et al., 2021) with two assisted ventilation modes, Neurally Adjusted Ventilator Assist (NAVA) and pressure support (PSV), for patient-specific respiratory drive estimation. The overall goal is estimate patient spontaneous effort with only non-invasive breath data and thus to ease burden on clinicians work and equipment cost, as well as technique trainings and problems coming behind. The outcome is compared with recorded EAdi signal and clear trends/correlations are observed.

2. METHODS

2.1 Patient Effort Estimation Model

This patient effort estimation model is based on the well-validated digital twin model in (Zhou, C., et al., 2021):

$$f_V(t) + PEEP = \ddot{V} + R\dot{V} + K_eV + K_{h1}V_{h1} + K_{h2}V_{h2} \quad (1)$$

where V is the volume of air delivered to the lungs ($\ddot{V}$ and $\dot{V}$ are the corresponding second and first derivatives of V), V_{h1} and V_{h2} are hysteretic volume response during inspiration and expiration, respectively, K_e represents the alveolar recruitment elastance, K_{h1} and K_{h2}, are determined by two nonlinear hysteretic springs for alveolar hysteresis elastance during inspiration and expiration, respectively, R is the airway resistance, and PEEP is the positive end-expiratory pressure. $f_V(t)$ is the steady-state input force (driving pressure over time) and identified at baseline PEEP level.

An additional negative term, $\hat{P}_p$, is added to represent pleural driving pressure and thus to estimate patient spontaneous effort (Knopp, J.L., et al., 2021):

$$P - PEEP = \ddot{V} + R\dot{V} + K_eV + K_{h1}V_{h1} + K_{h2}V_{h2} + \hat{P}_p \quad (2)$$

This $\hat{P}_p$ term is modelled using 2nd order (d = 2) b-spline functions with a knot width (k_w) of 0.05s to define the unknown, patient-specific $\hat{P}_p$:

$$\hat{P}_p = \sum_{i=1}^{M} -P_{s,i}\Phi_{i,2}(t) \quad (3)$$

Where $P_{s,i}$ are constant coefficients identified from measured data. $M = \frac{T_{insp}}{k_w} + d$ by b-spline functions setting. T_{insp} is the inspiration duration for each breath in seconds. The term $\Phi_{i,2}(t)$ using a 2nd order definition is calculated:

$$\Phi_{i,d}(t) = \frac{t - T_i}{T_{i+d} - T_i}\Phi_{i,d-1}(t) + \frac{T_{i+d+1} - t}{T_{i+d+1} - T_{i+1}}\Phi_{i+1,d-1}(t), d \geq 1$$

$$\Phi_{i,0}(t) = \begin{cases} 1, & T_i < t < T_i + 1 \\ 0, & otherwise \end{cases} \quad (4)$$

Where T_i are equally spaced division points in time calculated by $\frac{T_{insp}}{k_w}$. Finally, (1) can be defined (Knopp, J.L., et al., 2021):

$$P - PEEP = \ddot{V} + R\dot{V} + K_eV + K_{h1}V_{h1} + K_{h2}V_{h2} + \sum_{i=1}^{M} -P_{s,i}\Phi_{i,2}(t) \quad (5)$$

With ventilator breath data (airway pressure and flow), linear least squares regression can identify patient-specific, lung mechanics variables and $\hat{P}_p$ (by identifying the $P_{s,i}$ terms), using the Matlab (Mathworks, Natick, MA, USA) lsqlin function, and constraining elements of $P_{s,i} > 0$ ($\hat{P}_p$ negative) to ensure identifiability (Docherty, P.D., et al., 2011).

2.2 Analysis

22 patients under both NAVA and PSV are analyzed in this approach. Data from the same 20 breaths per patient under NAVA ventilation used in (Knopp, J.L., et al., 2021) are tested and outcomes are compared, thus analysing the differences between lung mechanics models employed. In addition, PSV data is also studied for each patient with the first 20 breaths, which was not used in previous work (Knopp, J.L., et al., 2021), providing a comparison between modes for the overall modelling approach.

2.2.1 Negative constraint on b-splines functions

This model currently only focuses on the inspiration phase of each breath, while originally the first 75% of identified $P_{s,i}$ parameters during inspiration are constrained to be positive ($\hat{P}_p$ negative) and the rest 25% is not constrained in previous study (Knopp, J.L., et al., 2021). This constraint is applied for each studied breath per patient and captures negative patient spontaneous effort and any patient resistance to ventilator action in the unconstrained portion.

In this study, the amount of values constrained are tested from 0%, 10%, …, 100%, where 0% represents free identification of $P_{s,i}$ values and likely identifiability issues, and 100% forces this term to be strictly negative capturing only breathing effort. An example plot for b-splines functions yielding $\hat{P}_p$ curve during inspiration phase is presented in Figure 1 with negative constraint for $-P_{s,i}$ is 70%.

2.2.2 EAdi signal analysis

Clinical EAdi signals available in this studied trial for both NAVA and PSV provide a reference for muscle action for inspiratory effort. In particular, peak EAdi and AUC[EAdi] capture measured metrics of inspiratory effort for comparison to model-based metric. Thus, collected EAdi signal offer the opportunity to assess the resulting model-based inspiratory breathing effort identified.

Note, since the studied $\hat{P}_p$ curves only focus inspiration phase to identify patient inspiratory effort, AUC[EAdi] is limited to inspiration phase to keep consistent, as presented in Figure 2.

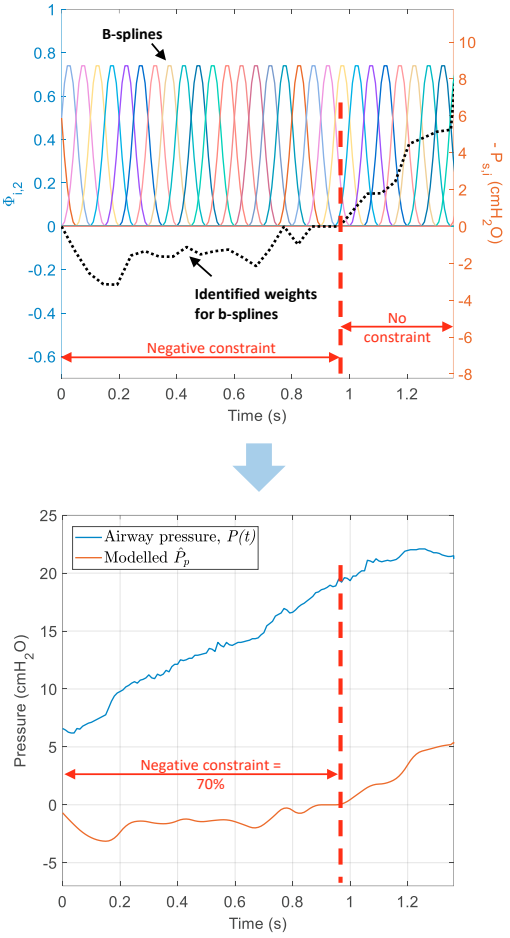

Figure 1. Identified weights ($-P_{s,i}$) for b-splines ($\Phi_{i,2}$) and yielded $\hat{P}_p$ curve with associated measured airway pressure, $P(t)$, during inspiration phase. Negative constraint is 70% for $-P_{s,i}$, b-splines.

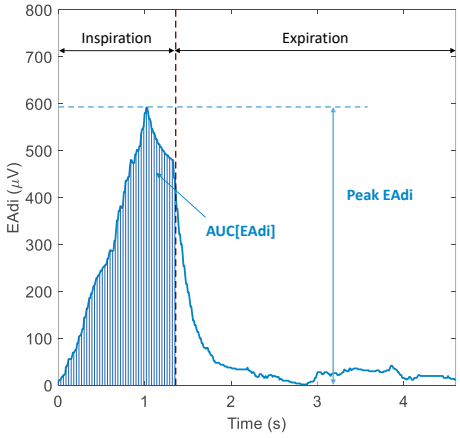

Figure 2. The analysed variables in EAdi signal over a complete breath.

2.2.3 $\hat{P}_p$ curve analysis

While $P_{s,i}$ values constraint level is adjusted and tested, $\hat{P}_p$ curve can have positive areas ($\hat{P}_p$ values > 0) and negative areas ($\hat{P}_p$ values ≤ 0). Thus, $\hat{P}_p$ curve is separated into positive and negative areas while the area is calculated as its product over time (denoted as AUC $[\hat{P}_p]_{pos}$ and AUC $[\hat{P}_p]_{neg}$), as presented in Figure 3. To note, AUC$[\hat{P}_p]_{neg}$ is calculated as a positive value without regard to its under-zero curve.

Finally, the area under the complete $\hat{P}_p$ curve (AUC$[\hat{P}_p]$) is calculated as the sum of AUC$[\hat{P}_p]_{pos}$ and AUC$[\hat{P}_p]_{neg}$, defined:

$$\mathrm{AUC}[\hat{P}_p] = \mathrm{AUC}[\hat{P}_p]_{neg} + \mathrm{AUC}[\hat{P}_p]_{pos} \quad (6)$$

Meanwhile, PRCT_{neg} is calculated as the percentage of AUC$[\hat{P}_p]_{neg}$ over AUC$[\hat{P}_p]$, capturing the percentage of work of breathing committed to inspiratory effort, defined:

$$PRCT_{neg} = AUC[\hat{P}_p]_{neg} / \mathrm{AUC}[\hat{P}_p] \quad (7)$$

Specially, to differentiate with the negative constraint for $P_{s,i}$, PRCT_{neg} is described in 0, 0.1, …, 1.0, while negative constraint for $P_{s,i}$ is described in 0%, 10%, …, 100%.

In this study, peak EAdi and AUC[EAdi] are analysed and the associated breaths are separated into two groups according to PRCT_{neg} values, while one group contains all breaths that have PRCT_{neg} < PRCT_{neg} limit and other group for PRCT_{neg} ≥ PRCT_{neg} limit. PRCT_{neg} limit is tested from 0, 0.1, …, 1.

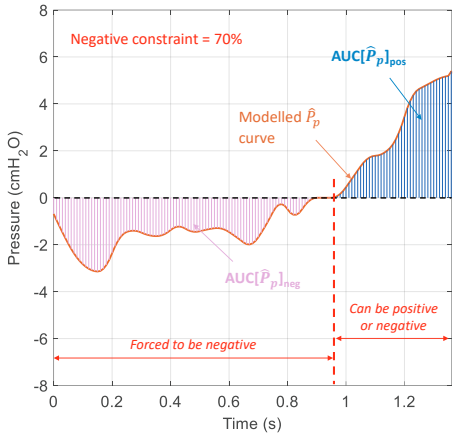

Figure 3. The analysed variables in $\hat{P}_p$ curve during inspiration phase of a breath.

3. RESULTS

3.1 Outcome with NAVA data

Figure 4 shows an example for peak EAdi values for tested breaths (440 breaths in total) grouped via PRCT_{neg} limit (0.1, 0.2, …, 0.9, 1.0), with a b-splines function constraint level of 50%. It can be seen lower peak EAdi breaths (≤ ~3000μV) tend to locate in PRCT_{neg} ≥ limit group, especially when PRCT_{neg} limit = 0.6-0.9. This performance can be observed with constraint levels of 30%-60%.

Correspondingly, Figure 5 shows the results for AUC[EAdi] with the same b-splines constraint level of 50%. The similar trend in peak EAdi outcome can be also observed in AUC[EAdi] (≤ ~2000μV*t) with constraint = 10%-60% and PRCT_{neg} limit = 0.5-1.0.

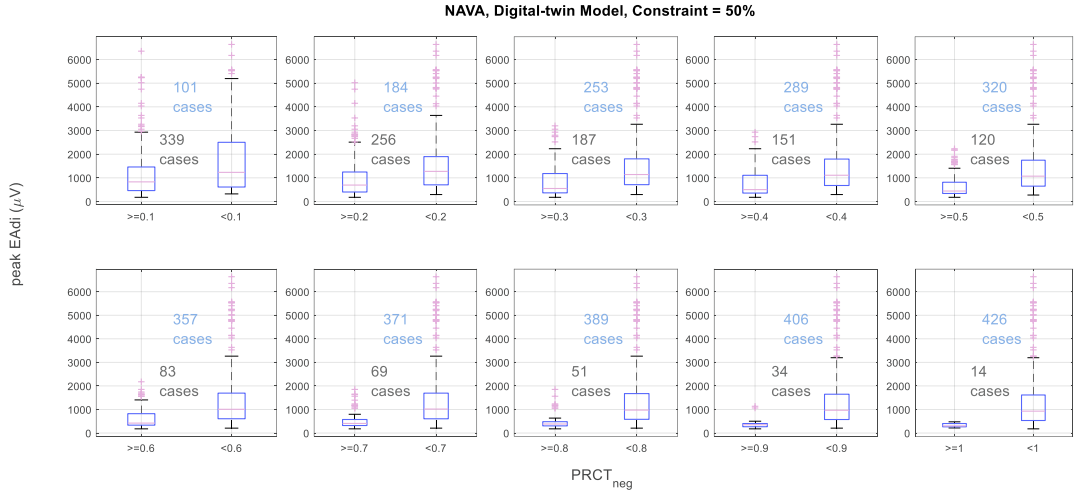

Figure 4. Peak EAdi values for tested breaths (440 breaths in total) grouped via $PRCT_{neg}$ limit (0.1, 0.2, …, 0.9, 1.0) with $\hat{P}_p$ negative constraint = 50%. Patient data under NAVA mode are used.

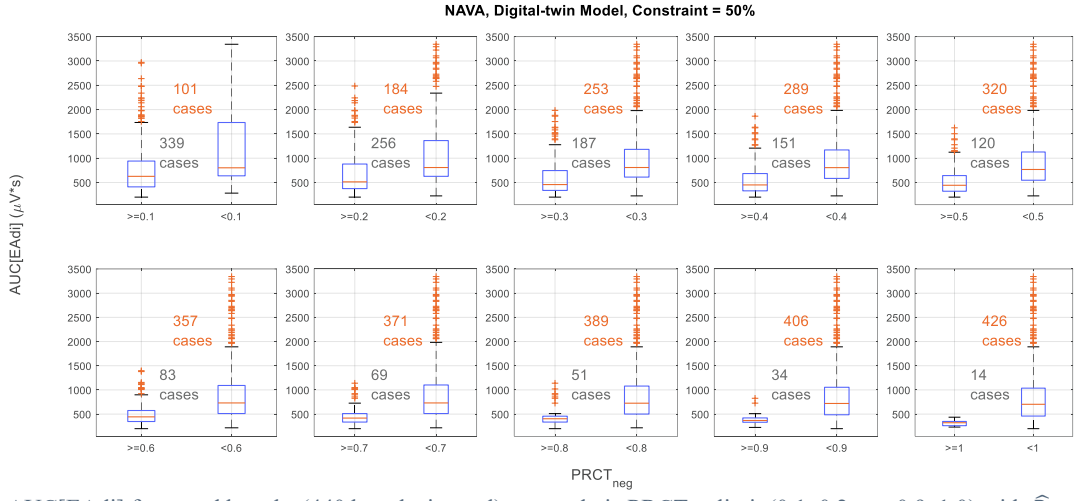

Figure 5. AUC[EAdi] for tested breaths (440 breaths in total) grouped via $PRCT_{neg}$ limit (0.1, 0.2, …, 0.9, 1.0) with $\hat{P}_p$ negative constraint = 50%. Patient data under NAVA mode are used.

Table 1 provides the correlation analysis with R^2 values among studied variables, $PRCT_{neg}$, AUC[$\hat{P}_p$]$_{neg}$, peak EAdi, and AUC[EAdi] while $\hat{P}_p$ negative constraint levels = 0%, 10%, …, 100% with NAVA data. Higher R^2 values are observed with $PRCT_{neg}$ versus AUC[EAdi] with constraint levels of 50%-90%.

Table 1. R^2 values (median [IQR]) for PRCTneg and AUC[$\hat{P}_p$]$_{neg}$ versus AUC[EAdi] and peak EAdi with $\hat{P}_p$ negative constraint levels = 0%, 10%, …, 100%. Patient data under NAVA mode are used.

$\hat{P}_p$ negative constraint level	R^2 values of			
	$PRCT_{neg}$ vs AUC[EAdi]	$PRCT_{neg}$ vs peak EAdi	AUC[$\hat{P}_p$]$_{neg}$ vs AUC[EAdi]	AUC[$\hat{P}_p$]$_{neg}$ vs peak EAdi
0%	0.19 [0.06 0.32]	0.12 [0.05 0.22]	0.02 [0.01 0.19]	0.04 [0.01 0.18]
10%	0.2 [0.08 0.37]	0.13 [0.06 0.23]	0.02 [0.01 0.21]	0.05 [0.01 0.18]
20%	0.19 [0.09 0.32]	0.15 [0.06 0.25]	0.02 [0.01 0.17]	0.04 [0.01 0.16]
30%	0.29 [0.15 0.42]	0.15 [0.07 0.33]	0.04 [0.01 0.17]	0.04 [0.02 0.1]
40%	0.37 [0.17 0.57]	0.2 [0.13 0.51]	0.04 [0.01 0.18]	0.04 [0.01 0.11]
50%	0.53 [0.19 0.64]	0.36 [0.21 0.61]	0.06 [0.03 0.28]	0.05 [0.01 0.19]
60%	0.5 [0.32 0.69]	0.45 [0.31 0.67]	0.09 [0.03 0.31]	0.06 [0.01 0.23]
70%	0.58 [0.36 0.74]	0.47 [0.33 0.65]	0.12 [0.04 0.33]	0.12 [0.02 0.24]
80%	0.58 [0.32 0.68]	0.50 [0.4 0.6]	0.16 [0.05 0.32]	0.17 [0.03 0.28]
90%	0.46 [0.34 0.6]	0.43 [0.37 0.59]	0.15 [0.04 0.37]	0.17 [0.03 0.31]
100%	0 [0 0]	0 [0 0]	0.17 [0.03 0.35]	0.14 [0.04 0.3]

3.2 Outcome with PSV data

Overall, the outcome with PSV is more variable compared with NAVA. To contrast, the R^2 values for PSV data are much

lower than NAVA data stated in Table 1, with a maximum median R^2 value of 0.21.

However, trends are still observed, differing only based on $PRCT_{neg}$ limits. Figure 6 presents the same analysis in Figure 4 for PSV data as an example. It can be seen when $PRCT_{neg}$ limit = 0.1-0.4, higher peak EAdi breaths tend to locate in $PRCT_{neg} \geq$ limit group. While $PRCT_{neg}$ limit ≥ 0.7, higher peak EAdi breaths tend to locate in $PRCT_{neg}$ < limit group, conversely.

For AUC[EAdi] analysis, with constraint levels of 30% and 40%, lower AUC[EAdi] (≤ ~2000μV*s) tends to locate in $PRCT_{neg} \geq$ limit group while $PRCT_{neg}$ limit = 0.3-1.0. However, with constraint levels of 50% and 60%, same trends are observed with $PRCT_{neg}$ limit = 0.4, while opposite trends (lower AUC[EAdi] tends to locate in $PRCT_{neg}$ < limit group) are observed with $PRCT_{neg}$ limit = 0.9-1.0.

In short, trends are observed for $PRCT_{neg}$ versus EAdi signal analysis for both NAVA and PSV data. The trend is consistent across $PRCT_{neg}$ limits in NAVA, while two trends are observed and being opposite for $PRCT_{neg}$ limit < 0.4 and $PRCT_{neg}$ limit ≥ 0.7 in PSV, which is thus more variable. This variability and the low correlation R^2 values ($\hat{P}_p$ curve versus EAdi signal) match other studies showing PSV did not match tidal volume and EAdi well.

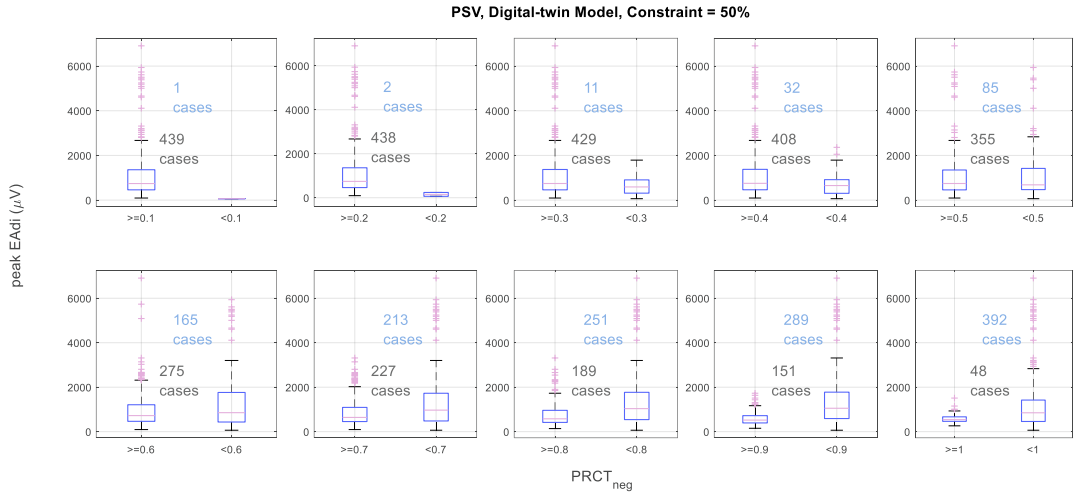

Figure 6. Peak EAdi values for tested breaths (440 breaths in total) grouped via $PRCT_{neg}$ limit (0.1, 0.2, …, 0.9, 1.0), while $\hat{P}_p$ negative constraint level = 50%. Patient data under PSV mode are used.

4. DISCUSSION

The negative area of $\hat{P}_p$ has been considered as representation for patient negative spontaneous breathing work in original approach (Knopp, J.L., et al., 2021). Considering it is a patient-specific and breath-specific variable, $PRCT_{neg}$ is analysed in Figures 4-6 and Table 1 for NAVA and PSV data.

An appreciable correlation for NAVA data is observed for $PRCT_{neg}$ versus AUC[EAdi], where a $\hat{P}_p$ negative constraint level of 70%, with a median R^2 value of 0.58 and IQR = 0.36-0.74 compared to R^2 values in (Knopp, J.L., et al., 2021) with median 0.55 and IQR = 0.38-0.70. The 60% and 80% constraint levels also offers similar or better performance, as presented in Table 1.

Then, Figure 4 as an example shows a trend that breaths have larger $PRCT_{neg}$ tend to yield lower peak EAdi values (≤ 3000μV), when $\hat{P}_p$ negative constraints = 30%-60%. Meanwhile, this trend is also found for $PRCT_{neg}$ versus AUC[EAdi] when constraint level is between 10%-60%. Therefore, for NAVA data, the 60% $\hat{P}_p$ negative constraint level yielded the overall best compromise, with strong correlation between peak EAdi and $\hat{P}_p$ values and physiologically-relevant meaning for $\hat{P}_p$ curve negative area.

Compared with NAVA ventilation, which allows proportional assist basing on measured EAdi signals, PSV simply delivers airway flow up to a targeted driving pressure (peak inspiratory pressure - PEEP). There is thus significant mismatch for many patients between inspiratory effort measured by EAdi and the tidal volume achieved (Chiew, Y., et al., 2013, Chiew, Y.S., et al., 2011, Moorhead, K., et al., 2013, Piquilloud, L., et al., 2011). This mismatch is expected to yield a correspondingly lower correlation between inspiratory effort identified, or measured via EAdi, and outcome work of breathing or tidal volume.

The correlations with PSV data all resulted in lower R^2 values than NAVA outcome, with maximum median R^2 value of 0.21 to 0.58. However, trends observed between EAdi signals and $PRCT_{neg}$ for NAVA, Figures 4 and 5, can still be observed in PSV while being relatively more variable. The results match expectations from prior studies (Chiew, Y., et al., 2013, Chiew, Y.S., et al., 2011, Moorhead, K., et al., 2013), and as a result of observed poorer patient-ventilator interaction (Piquilloud, L., et al., 2011). The variability between patients is based on how well NAVA and PSV provided good patient-ventilator matching and interaction (Chiew, Y., et al., 2013, Chiew, Y.S., et al., 2011, Moorhead, K., et al., 2013).

Overall, physiologically-relevant correlations in $\hat{P}_p$ curve negative area and EAdi signal can be found in both NAVA and PSV data analysis. A $\hat{P}_p$ negative constraint level of 40-70% is required to ensure identifiability and physiological relevance in comparison to measured inspiratory effort in the studied

trial. Results differ between NAVA and PSV modes based on the poorer patient-ventilator interaction observed in PSV, and these trends are patient-specific. Moreover, basing on previous studies for digital-twin model in lung mechanics identification and prediction in other mechanical ventilation (MV) modes (Sun, Q., et al., 2021, Sun, Q., et al., 2022, Zhou, C., et al., 2021), this approach is promising in wider use in clinical. More clinical trials and data are required for further studies.

5. CONCLUSION

In conclusion, the proposed b-spline estimation method for inspiratory effort functions well for both NAVA and PSV data. Physiologically-relevant information is found within the identified $\hat{P}_p$ curve for both NAVA and PSV modes, which could be used to help guide weaning or changes in MV mode settings. Further, its efficacy for the digital-twin model is promising for creating a more general overall model-based approach to personalised and predictive MV monitoring and care. In future, the identified $\hat{P}_p$ could potentially be used to replace the need for costly measurement of EAdi signals in these clinically common MV patients.

REFERENCES

Akoumianaki, E., Maggiore, S.M., Valenza, F., Bellani, G., Jubran, A., Loring, S.H., Pelosi, P., Talmor, D., Grasso, S., Chiumello, D., Guérin, C., Patroniti, N., Ranieri, V.M., Gattinoni, L., Nava, S., Terragni, P.-P., Pesenti, A., Tobin, M., Mancebo, J. and Brochard, L. (2014). The Application of Esophageal Pressure Measurement in Patients with Respiratory Failure. *American Journal of Respiratory and Critical Care Medicine,* 189**,** 520-531.

Albani, F., Pisani, L., Ciabatti, G., Fusina, F., Buizza, B., Granato, A., Lippolis, V., Aniballi, E., Murgolo, F., Rosano, A., Latronico, N., Antonelli, M., Grasso, S. and Natalini, G. (2021). Flow Index: a novel, non-invasive, continuous, quantitative method to evaluate patient inspiratory effort during pressure support ventilation. *Critical Care,* 25.

Chiew, Y., Chase, J., Lambermont, B., Roeseler, J., Pretty, C., Bialais, E., Sottiaux, T. and Desaive, T. (2013). Effects of Neurally Adjusted Ventilatory Assist (NAVA) levels in non-invasive ventilated patients: titrating NAVA levels with electric diaphragmatic activity and tidal volume matching. *BioMedical Engineering OnLine,* 12**,** 61.

Chiew, Y.S., Piquilloud, L., Desaive, T., Lambermont, B., Roeseler, J., Revelly, J., Bialais, E., Tassaux, D., Jolliet, P. and Chase, J. (2011). Effect of various Neurally adjusted ventilatory assist (NAVA) gains on the relationship between diaphragmatic activity (Eadi max) and tidal volume. *24th Annual Congress of the European Society of Intensive Care Medicine (ESICM 2011).* Berlin, Germany.

Docherty, P.D., Chase, J.G., Lotz, T.F. and Desaive, T. (2011). A graphical method for practical and informative identifiability analyses of physiological models: a case study of insulin kinetics and sensitivity. *Biomed Eng Online,* 10**,** 39.

Doorduin, J., van Hees, H.W.H., van der Hoeven, J.G. and Heunks, L.M.A. (2013). Monitoring of the Respiratory Muscles in the Critically Ill. *American Journal of Respiratory and Critical Care Medicine,* 187**,** 20-27.

Jansen, D., Jonkman, A.H., Roesthuis, L., Gadgil, S., van der Hoeven, J.G., Scheffer, G.-J.J., Girbes, A., Doorduin, J., Sinderby, C.S. and Heunks, L.M.A. (2018). Estimation of the diaphragm neuromuscular efficiency index in mechanically ventilated critically ill patients. *Critical Care,* 22**,** 238.

Jonkman, A.H., de Vries, H.J. and Heunks, L.M.A. (2020). Physiology of the Respiratory Drive in ICU Patients: Implications for Diagnosis and Treatment. *Critical Care,* 24**,** 104.

Knopp, J.L., Chase, J.G., Kim, K.T. and Shaw, G.M. (2021). Model-based estimation of negative inspiratory driving pressure in patients receiving invasive NAVA mechanical ventilation. *Comput Methods Programs Biomed,* 208**,** 106300.

Moorhead, K., Piquilloud, L., Lambermont, B., Roeseler, J., Chiew, Y., Chase, J.G., Revelly, J.-P., Bialais, E., Tassaux, D., Laterre, P.-F., Jolliet, P., Sottiaux, T. and Desaive, T. (2013). NAVA enhances tidal volume and diaphragmatic electro-myographic activity matching: a Range90 analysis of supply and demand. *Journal of Clinical Monitoring and Computing,* 27**,** 61-70.

Piquilloud, L., Vignaux, L., Bialais, E., Roeseler, J., Sottiaux, T., Laterre, P.-F., Jolliet, P. and Tassaux, D. (2011). Neurally adjusted ventilatory assist improves patient–ventilator interaction. *Intensive Care Medicine,* 37**,** 263-271.

Sun, Q., Chase, J.G., Zhou, C., Tawhai, M.H., Knopp, J.L., Möller, K. and Shaw, G.M. (2021). Over-distension prediction via hysteresis loop analysis and patient-specific basis functions in a virtual patient model. *Computers in Biology and Medicine,* 141**,** 105022.

Sun, Q., Chase, J.G., Zhou, C., Tawhai, M.H., Knopp, J.L., Möller, K. and Shaw, G.M. (2022). Non-invasive over-distension measurements: data driven vs model-based. *Journal of Clinical Monitoring and Computing*.

Telias, I., Junhasavasdikul, D., Rittayamai, N., Piquilloud, L., Chen, L., Ferguson, N.D., Goligher, E.C. and Brochard, L. (2020). Airway Occlusion Pressure As an Estimate of Respiratory Drive and Inspiratory Effort during Assisted Ventilation. *American Journal of Respiratory and Critical Care Medicine,* 201**,** 1086-1098.

Telias, I. and Savino, S. (2019). Techniques to monitor respiratory drive and inspiratory effort. *Current Opinion in Critical Care,* 26**,** 1.

Vargas, M., Buonanno, P., Sica, A., Ball, L., Iacovazzo, C., Marra, A., Pelosi, P. and Servillo, G. (2022). Patient-Ventilator Synchrony in Neurally-Adjusted Ventilatory Assist and Variable Pressure Support Ventilation. *Respir Care,* 67**,** 503-509.

Zhou, C., Chase, J.G., Knopp, J., Sun, Q., Tawhai, M., Möller, K., Heines, S.J., Bergmans, D.C., Shaw, G.M. and Desaive, T. (2021). Virtual patients for mechanical ventilation in the intensive care unit. *Computer Methods and Programs in Biomedicine,* 199**,** 105912.